International Journal of Multidisciplinary Research and Development
Online ISSN: 2349-4182, Print ISSN: 2349-5979, Impact Factor: RJIF 5.72
www.allsubjectjournal.com
Volume 4; Issue 7; July 2017; Page No. 97-105

Effect of impingement heights on temperature time cooling curve on a run-out table system

[1] TO Onah, [2] AO Odukwe, [3] SN Ojobor

[1] Dept. of Mechanical and Production Engineering, Enugu State University of Science and Technology Enugu, Enugu, Nigeria
[2] Professor, Department of Mechanical Engineering, University of Nigeria Nsukka, Enugu, Nigeria
[3] Professor, Department of Mechanical Engineering, Caritas University Amorji Nike Enugu, Enugu, Nigeria

Abstract
This research focuses on the development of controlled accelerated top water jet cooling model and water flow to characterize heat extraction on hot steel plates. The methodology undertaken for this research involved design and construction of an experiments using a pilot scale run-out table with stationary plates in MMLE ESUT, Nigeria. Both initial hot plate and water temperatures, control cooling time, controlled temperature ranges of 160^0C to 200^0C, and 260^0C to 300^0C, pressure, volumetric flow rates, impingement water jet 0.8mm of 30 number holes, nozzles to surface spacing of 40mm 50mm, 60mm and 70mm, and pipe diameters of 20mm, 25mm, 32mm and 45mm were parameters investigated. Experimentally, three k-type thermocouples were instrumented and installed 9mm from the bottom surface of the plate. Temperature measurements were taken at impingement target on where convectional and evaporation cooling occurred. Conduction heat transfer modelling allowed the calculation of zero temperature. Transient state temperature across the work piece was done by Visual Basic Heat Transfer (VBHT) model. From transient cooling data obtained, studies on effect of impingement height showed that optimum cooling occurred at smaller pipe diameter of 20mm at impingement height of 70mm and bigger pipe diameter of 45mm at impingement height of 40mm at controlled cooling temperature of 300^0C because use of the stream wise velocity.

Keywords: run–out table pilot scale plant, impingement heights, pipe diameters, temperatures and transient heat transfer

1. Introduction
Steel companies that aim to produce steel plates of various qualities and thicknesses invariably start by re-heating steel slabs from the continuous –casting plant to rolling temperatures of about 900ºC. This is then followed by passing the re-heated slabs through a number of rolling-stands. Subsequently, the rolled plates are cooled, on lines, on the run-out table.
Controlled accelerated cooling on the run-out table of a hot rolling mill is a key technology to achieve the microstructure and properties of advanced steels. The increased demands for hot rolled products for severe service conditions have led to high interest in advanced steel grades. Accelerated but controlled cooling in the run-out table enables phase transformation of the product and enhanced metallurgical properties hitherto achieved by expensive alloying.
Thus, it is crucial to develop accurate heat transfer models in order to predict the temperature history of the steel plates on run-out tables. This study describes a strategy to develop a controlled accelerated cooling model to stimulate the temperature of the plate cooled by top water jet nozzle on a run-out table. Systematic experiments were carried out on a pilot scale run-out table facility using planar (water curtain) nozzle. Proposed experimental results for cooling of stationary plate, showed that the heat transfer rate depends strongly on the distance from the jet especially in the temperature range where the transition boiling regime occurs. With the experimental results, a boiling curve model is proposed that would take into account boiling heat transfer mechanism and maps local boiling curve for cooling of stationary steel plates. The effects of heat by boiling, heat by conventional cooling and heat by conduction during water flow rate and water temperature on the heat extraction from the plates were used to form the model.
Then, parametric experimental heat transfer studies were conducted to investigate the effect of impingement heights, the effect of pipe nozzle diameters. Also, transient heat conduction within the plate were analyzed and surface heat flux, convective heat transfer, boiling heat transfer. The validity of the cooling model will be examined with multiple nozzles experimental data from the literature.

1.1 Heat transfer mechanism on the run-out table
Since the temperature of the steel on the run-out table is higher than the boiling temperature of the water impinging on the surface, the dominant mode of heat transfer is jet impingement boiling. The latent heat of evaporation and high specific heat capacity of water allow high rates of heat extraction from the hot steel during cooling.
The boiling curve is the most descriptive representation of surface heat transfer changes during cooling of a hot solid by a liquid. The boiling curve presents heat flux changes with respect to the surface temperature of the solid. This curve is shown qualitatively in fig.1 for pool boiling. Pool boiling occurs when a hot surface is submerged in a pool of liquid, whereas forced flow boiling refers to the condition in which liquid flows over the surface (Dhir 1998, Tong and Tang 1997). Although the boiling heat transfer observed during run-out table cooling is categorized as forced flow boiling (Wolf *et al*., 1993), a pool boiling curve offers the fundamental groundwork for understanding boiling heat transfer in general. Four main regimes occur during pool

boiling: single-phase convection (natural convection), nucleate boiling, transition boiling, and film boiling (Dhir 1998, Wolf *et al*., 1993, Tong and Tang 1997).

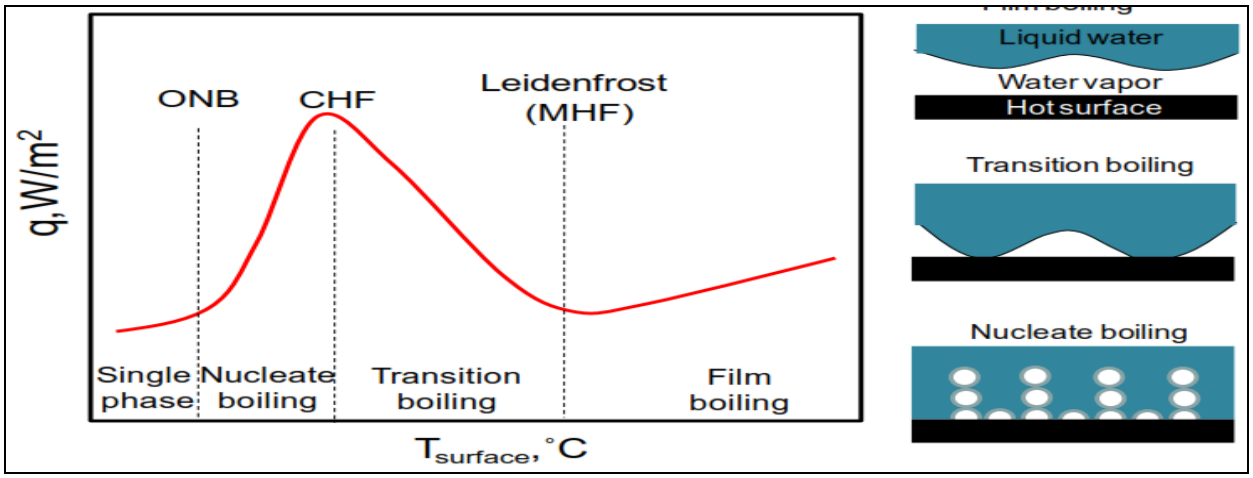

Fig 1: Schematic drawing of a typical pool boiling curve

At low temperatures (below saturation temperature), the water is heated by natural convection. This regime is single-phase convection since no vapor forms and no boiling occurs. At a temperature slightly above the saturation temperature, isolated vapor bubbles begin to form on the surface. This temperature is shown as ONB (onset of nucleate boiling) in fig. 1 and this boiling regime is called partial nucleate boiling. Partial nucleate boiling is characterized by a dynamic formation, growth and collapse of isolated vapor bubbles on the surface. The latent heat of evaporation and also the induced agitation due to the dynamics of bubbles increase the surface heat flux. With a further increase in temperature the bubble population increases leading to the transition from partial nucleate boiling to fully developed nucleate boiling. It has been observed that in this mode, isolated bubbles begin to merge in the vertical direction and the vapor leaves the surface in the form of jets. Bubbles also merge in the horizontal direction forming occasional vapor patches. However, as the population of the bubbles further increases, the more frequent vapor patches obstruct the path of incoming liquid to the surface thereby decreasing the heat transfer rate. Due to this fact, a maximum in the heat flux curve appears, termed the critical heat flux (CHF). The maximum or CHF represents the upper limit of nucleate boiling heat flux and the termination of efficient cooling conditions on the surface (Dhir 1998).

After the CHF point, the surface is covered alternately either by a vapor blanket or a liquid layer. In this regime, called transition boiling, vapor begins to cover larger portions of the surface due to the high evaporation rate. Since the thermal conductivity of the vapor is much lower than that of the water, the vapor acts as an insulating layer and decreases the heat transfer rate from the surface. Hence, in this regime the heat flux decreases with increasing surface temperature until the entire affected surface is covered by a blanket of vapor. At this point, liquid no longer wets the surface of the solid and a minimum heat flux (MHF) is reached in transition boiling region, which is the "Leiden frost" point. The condition after the stable vapor blanket has formed is referred to as film boiling. In film boiling, heat must be conducted mainly through the vapor blanket before it reaches the liquid, until radiation becomes the dominant mechanism at higher surface temperatures. Despite significant effort to simulate accelerated cooling, it is challenging to accurately incorporate fundamental boiling mechanisms into the transient heat transfer models for the run- out table. This is due to the fact that different boiling regimes are simultaneously occurring at different locations on the surface of the steel during jet impingement cooling. The cooling process is further complicated by the dependency of heat transfer regimes on process parameters such as nozzle geometry, water flow rate and water temperature. Moreover, on the run-out table, jet impingement cooling involves surface motion and interaction between neighboring water jets. (Filipovic *et al.*, 1994b, Timm *et al*., 2002).

2. Materials and Methodology

2.1 Experimental Set –Up For Pilot Scale Plant Run Out Table

In this research, a pilot scale run out table (ROT) facility was designed and constructed in Mechanical and Metallurgical Engineering Foundry Laboratory (MMEFL), ESUT. A schematic diagram of the run-out table and picture of the set-up in fig.2

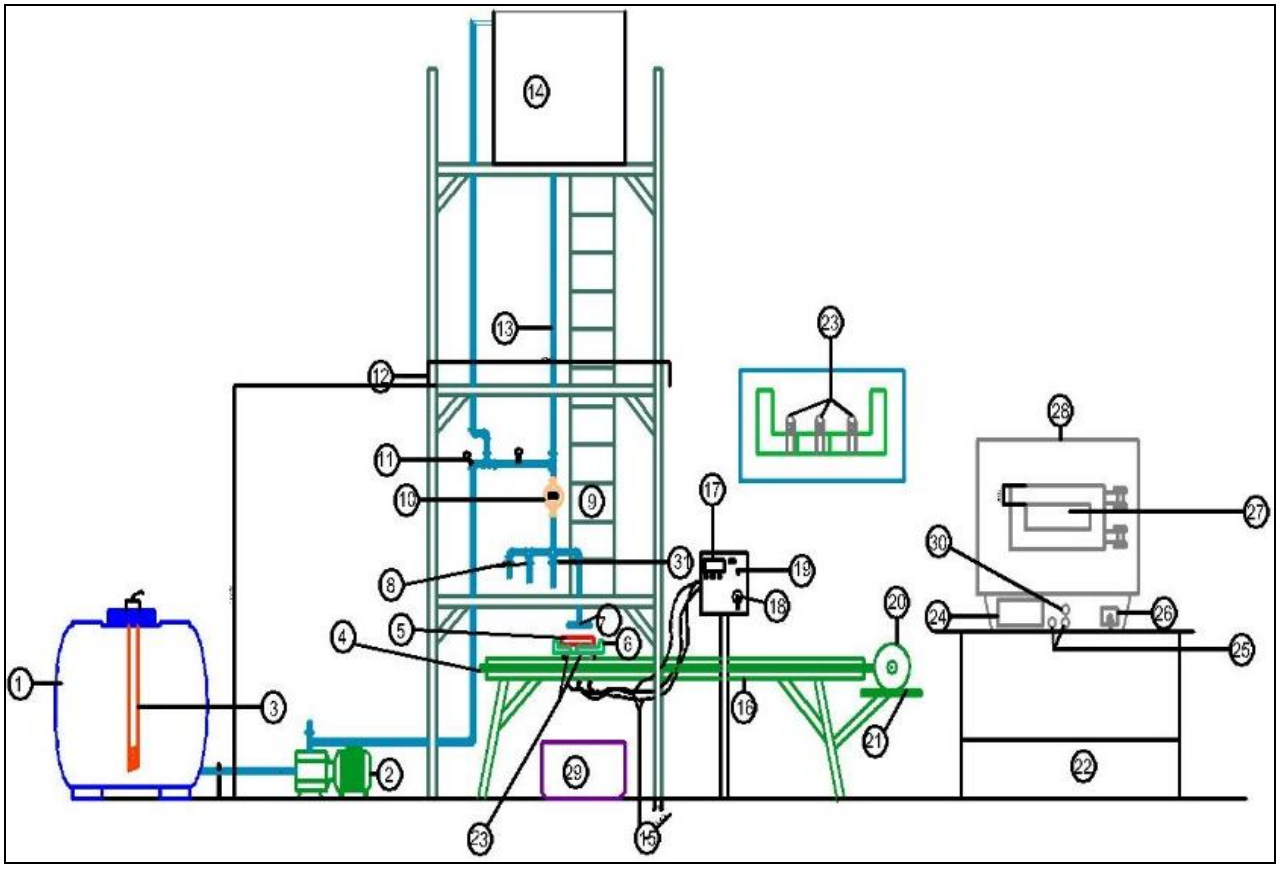

Fig 2: Schematic diagram of pilot plant for this research in MMEFL
1. Water tank, 2. Electric pump, 3.Heater, 4.Conveyor screw, 5.Work piece, 6.Work piece bed, 7.Impingement nozzle, 8.Ball gauge socket, 9.Ladder, 10.Flow meter, 11.Pressure meter, 12.Tower, 13.PVC pipe, 14.Reservoir, 15.Thermocouple wire, 16.Motorized Screw conveyor, 17.Thermocouple control panel, 18.Regulator, 19.Lock, 20.Electric motor, 21.Electric motor support, 22.Furnace support, 23.Thermocouple, 24.Furnace indicator, 25.Furnace switch, 26.Furnace regulator, 27.Furnace door, 28.Electric furnace, 29.Water collector, 30.Pilot light Header.

The facility has been designed to simulate industrial cooling condition for run-out table cooling of stationary plates in hot strip and plate mills (Prodanovic *et al.,* 2004). It enables heat transfer to be studied during cooling of stationary plates. In this study heating was provided by an electric furnace where a steel plate was heated up to a temperature of 920^0C in Metallurgical and Material Laboratory ESUT Enugu, Nigeria. Fusing a motorized ASYNCHRONE ROTOR gear powered conveyor drive system of 0.75kw of 1500rpm to operate a gear of 1:24 by ratio with 50HZ under an ac. of 240volts, the steel plates were transported from the furnace to the cooling tower for the stationary experiments.

The cooling system features a closed water loop where $0.945m^3$ (945 liters) of water was circulated throughout the experiment through the cooling jet nozzles. Surface temperatures, water temperatures, impingement heights or nozzle–to- surface spacing (impingement height) and flow rates were controlled. An ATLAS (ATP 60) water pump that provided total water flow rates of 60L/min was employed. It pumped water to the impingement plate from the water tank below to the target plate through the flow meter, nozzle header via impingement jet nozzle to the hot plate. An electric heater of 9kw of 330volts was situated in the tank and was used to adjust the temperature of water between 10-70^{o}C.The water temperatures readings were taken by a mercury in bulb thermometer.

In this study, one type of nozzle was used; planar (water or curtain) nozzle. The cross section is 12x 12 mm of 30 × 90mm with 0.8 mm with 30 number holes of jet diameter. A control panel mounted on a stand was used to read the surface temperatures of steel before and after the impingement. It has a red icons buttons that controls and records the temperature variations with digital read out on a steel cased panel.

2.2 Workpiece chemical composition test

Carbon steel is selected for the present experiment. The typical chemical composition of the sample steel plate shown in the table 1 indicates that test sample is a low carbon steel that has a melting point of 1600^{o}C. The process employed was electrode spark method, carried out with Electrode Spark Equipment method by Angstrom V-aso Spectrometer, Eastern Metal's Limited Asaba, Delta State Nigeria.

Table 1: Chemical composition of medium carbon steel (MCS)

Steel chemical composition	Fe	C	Si	Mn	S	P	Cr	Ni	Mn	Cu
Wt. %	98.480	0.25	0.095	0.755	0.042	0.010	0.053	0.051	0.016	0.103
Steel chemical composition	Al	V	Cu	Sn	As	Nb	Pb	W	B	
Wt. %	0.008	0.011	0.011	0.0377	0.010	0.000	0.000	0.050	0.0001	

2.3 Experimental procedure

After the required temperature of 920°C was reached in the electric furnace, the workpiece was removed and kept on the motorized screwed conveyor that transported the plate towards the cooling jet impingement target. For the experiment, the center of the plate was positioned under the jet nozzle, and the water flow from tank was started. The water header was positioned for different flow of water using different water pipe diameters and heights. The pressure gauge and flow meter were also opened to read the values of pressure and flow rate with stop watch. However, the initial surface temperatures of the plate (Ti) at the onset of water impingement cooling varied from 450 to 550°C. Temperature data of various thermocouple locations were collected when the surface temperature drops below 3°C of the three thermocouples and average initial or surface temperature was recorded. When the controlled impingement cooling reached 200°C, 180°C, 160°C and 300°C, 280°C and 260°C respectively, the flow was stopped using stop watch. The evaporated water was gotten, by subtracting volume of water collected from volume of water used, using flow meter and measuring cylinder.

2.4 Experimental sequence

Experiments were made at several water flow rates via flow meter to target heated plates. The procedures are sequentially explained below: I turned on the water supply to the flow line via flow meter to the hot plate through the header and various pipe diameter cum jet nozzle. Also turned was made on the heater to vary the water temperature using 9KN of electric heater. And read these parameters.

The sequence of experimental operation went like this: I monitored the reading until steady state nearly isothermal condition is achieved i.e. T_1, T_2, T_3 are with 0.5% of each other and took the average surface temperature of $\pm$3°C. Thereafter, I took final reading for particular flow rate of water say Q_1 of 20mm diameter with nozzle to surface height of 40mm. Then I repeated the experiment with another three set of 25mm, 32mm, 45mm diameters and 40mm, 60mm and 70mm impingement heights each for different controlled temperature cooling of 160 to 200°C and 260 to 300°C respectively. After each flow of impingement water then I changed D and H and repeated as above.

3. Heat transfer model

Evaluating the transient state temperature development across the work piece width of 120mm.

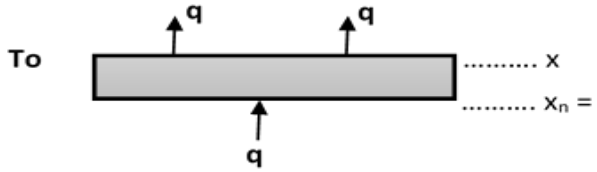

Fig 3: Sketch of energy balance

3.1 Boundary condition

The boundary conditions are to be applied at the top (surface of water jet impingement) and the bottom surfaces.

At the top surface; the boundary condition is solved using the energy balance of heat by conduction to be equals heat by convection and that by boiling:

$$q_k = q_c + q_b \quad (1)$$

where $q_k = -k\frac{\partial T}{\partial x})x_0$ = conductive heat transfer,kJ

$q_c = h(T_o - T_\infty)$=convective heat transfer KJ and

$q_b = mh_{fg}$ =heat out flow due to evaporation of cooling water KJ.

Thus, $-k\frac{\partial T}{\partial x})x_0 = q_k = h(T_o - T_\infty) + mh_{fg}$ (2)

Where k = thermal conductivity of the fluid (water) in w/m,k

∂T = change in temperature °C

∂x = division across the width of the workpiece in mm

h = coefficient of convective heat transfer in w/m^2k

$T_o - T_\infty$ = change in zero temperature and temperature of the immediate environment of the test plate °C

m = mass of water in Kg

h_{fg} = latent heat of vaporization of saturated water in KJ/kg

3.2 Discretization of temperature development

Using the transient – state discretization of temperature across the workpiece for 1 –D heat treatment on the workpiece. At the bottom surface, the heat is assumed to be constant. Thus, the temperature at all points are the same

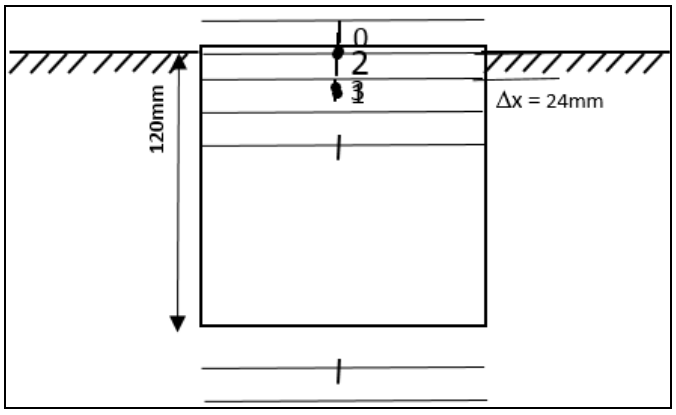

Fig 4: Discretization of transient state temperature development across the workpiece from 0 to n+1

The B.C at the bottom face: - The condition is approximated to an adiabatic bottom face (i.e. no heat lost to the workpiece supporting structure).

Using Taylor series expansion alouds T_o;

$$T_1 = T_o + \frac{\partial T}{\partial x})_o \Delta x + \frac{\partial^2 T}{\partial x^2}\frac{(\Delta x)^{2-}}{2_!} + \quad (3)$$

$$\therefore \quad \frac{\partial T}{\partial x})_o \Delta x = (T_1 - T_0)\frac{\partial^2 T}{-\partial x^2})_o \frac{(\Delta x)^{2-}}{21} \quad (4)$$

Or $$\frac{\partial T}{\partial x})_o \triangleq \frac{T_1 - T_o}{\Delta x} \quad (5)$$

Substituting equations (5) into (1),using equation 1.

Thus $$q_k = -k(T_1 - T_o)/_{\Delta x} \quad (6)$$

For $q_k = q_c + q_b$

Therefore,

$$-k\left\{\frac{T_1 - T_o}{\Delta x}\right\} = h\,(T_o - T_\infty) + q_b$$

$$-k\{T_1 - T_o\} = h\Delta x\,(T_o - T_\infty) + \Delta x\, q_b$$

$$T_1 - T_o = -\frac{h}{k}\Delta x\,(T_o - T_\infty) - \frac{\Delta x}{k} q_b$$

$$\therefore \quad T_o = T_1 + \frac{h}{k}\Delta x\,(T_o - T_\infty) + \frac{\Delta x}{k} q_b \qquad (7)$$

Solving for real T_o, ie

$$T_o = T_1 + \frac{h\Delta x}{k} T_0 - \frac{h\Delta x}{k} T_\infty + \frac{\Delta x q_b}{k}$$

$$T_0 - \frac{h\Delta x}{k} T_0 = T_1 - \frac{h\Delta x}{k} T_\infty + \frac{\Delta x q_b}{k}$$

$$\therefore T_o = \frac{k}{k - h\,\Delta x}\left\{\frac{T_1 k - h\Delta x T_\infty}{k}\right\} + \frac{k}{k - h\,\Delta x}\left\{\frac{\Delta x q_b}{k}\right\}$$

$$T_o = \frac{T_1 K - h\Delta x T_\infty}{K - h\Delta x} + \frac{\Delta x q_b}{k - h\Delta x} \qquad (8)$$

$$T_0 = \frac{T_1 K - h\Delta x T_\infty + \Delta x q_b}{K - h\Delta x} \qquad (9)$$

$T_\infty = 45^0$C is the temperature of the immediate environment of the test plate which could be as high as the superheated temperature of the evaporated steam.

But $q_b = mh_{fg}$, from equation 2, where $\dot{m}$ = mass of water lost due to evaporation.

$\dot{m} = \rho V$, where ρ = density of water = 1000kg/m^3, V = volume of evaporated water, from experimental values, h_{fg} = latent heat of vaporization of saturated water at 1 atm = 2257KJ/Kg (Kyle,B.G.,2000).

It is proposed to estimate the volume of evaporated water by subtracting unevaporated water from volume of water used.

Thus for,

$$T_0 = \frac{T_1 K - \Delta x(hT_\infty - q_b)}{K - h\Delta x} \qquad (10)$$

$$T_0 = \frac{T_1 K - \Delta x(hT_\infty - mh_{fg})}{K - h\Delta x} \qquad (11)$$

$$T_0 = \frac{T_1 K - \Delta x(hT_\infty - \rho V h_{fg})}{K - h\Delta x} \qquad (12)$$

For $q_b = mh_{fg}$, Thus, q_{bn} = 1000 x V x 2257

$$= 2257000VKJ/m^3 \qquad (13)$$

The various evaporated values of V are obtained from the experimental tables of 2, 3, 4, and 5 respectively.

Equation 12 therefore yields equation 14:

$$T_0 = \frac{T_1 K - \Delta x(hT_\infty - 2257000V)}{K - h\Delta x} \qquad (14)$$

3.3 Convection model calculations

The value of h is to be estimated from Lui and Wang, (2001)

$$Nu = \frac{hD}{k} = \sqrt{2}\, Re^{\frac{1}{2}} * Pr^{\frac{1}{6}} * \left(\frac{k_v}{k_L}\right)^{\frac{1}{2}} * \left(\frac{\Delta T_{Sub}}{\Delta T_{Sat}}\right)^{\frac{1}{2}} \qquad (15)$$

(Lui and Wang, 2001)

Where Nu is Nesselt Number, h is convective heat transfer coefficient (w/m^{2}k),k is thermal conductivity of steel (w/mk), D is the nozzle jet diameter (mm),Re is Reynolds Number, k_v and k_i are thermal conductivities of vapour and liquid (W/m^{o}C), respectively. ΔT_{sat} is the surface superheat which is the difference between the surface temperature and saturation temperature (boiling temperature of water). In the above equations ΔT_{sub} which is called subcooling is the difference between liquid temperature and saturation temperature.

At the end of the experimental run, during which the total amount of water impinged has been estimated and the non-evaporated also estimated, the evaporated may be estimated as the difference, and an average over time computed and used to calculate the quantity of mass transfer during the poll boiling or evaporation.

3.4 Calculation for the ratio of thermal conductivities of vapour and liquid

The thermal conductivity ratio of vapour and liquid is calculated from equation 16 below,

$$\left(\frac{k_v}{k_L}\right)^{\frac{1}{2}} \qquad (16)$$

Where K_v and K_L are thermal conductivities of vapour and liquid at various temperatures respectively

$$\left(\frac{k_v}{k_L}\right)^{\frac{1}{2}} \text{ at } 200^0\text{c} = \left(\frac{0.0401}{0.663}\right)^{1/2} = 0.0605 \qquad (17)$$

Thus $\left(\frac{k_v}{k_L}\right)^{\frac{1}{2}}$ at 200^0C $= (0.0605)^{1/2}$ (18)

3.5 Calculation for Prandtl Number (Pr)

The Prandlt Number Pr is calculated from the equation below as;

$$\Pr = \frac{Cp\mu}{k} \qquad (19)$$

Where Cp is the specific heat capacity of the liquid (water) (J/Kg.K) = 4500 J/KgK.

μ is the dynamic viscosity of liquid (water) (Kg/m.s) = $0.122x10^{-3}$Kg/m.s,

K is the thermal conductivity of liquid (water) = 0.663w/m.k

(J. V. Sergners and J.T.R Watson, 2005)

Thus, $\Pr = \frac{4500x0.12210^{-3}}{0.663}$ =0.910 at 200^0C (20)

3.6 Calculation for Reynolds Number (Re)

The values of Reynolds Numbers are obtained from equation (21) below,

$$\text{Re}= \frac{\rho VD}{\mu} = \frac{v_{jet}D}{\nu} \quad (21)$$

Where $\rho_{liquid(water)}$=1000kg/m^2 which is the density of water.

V_{jet} is the velocity of water jet from the calculated flow rate using $\frac{Q_n}{n}$ for n number of holes,

Where Q_n is the flow rates which is the quantity of water used per time (m^3/s),

n is the number of nozzle jet =30 number holes of 0.8mm each.

D is the diameter of the jet nozzle which is 0.0008m,

μ is dynamic viscosity = 0.567 × 10^{-3} kg/m. s,

ν is the kinematic viscosity=0.573 × 10^{-6}m/s by interpolation. *(John Wiley and Sons, Inc.,2012)*

But $V_j = \frac{Q_{jet}}{A}$ (22)

$$Q_{jet} = \frac{Q_{flow\ rate}}{30} \quad (23)$$

$$A = \frac{\pi D^2}{4} = \frac{3.142 \times 0.0008^2}{4} = 5.027\times10^{-7}\text{m}^2 \quad (24)$$

Also $V_j = \frac{Q_{jet}}{A} = \frac{\frac{Q_{flow\ rate}}{30}}{\frac{\pi D^2}{4}}$

$$= \frac{4Q}{30\ x\ \pi\ x\ 0.0008^2} = \frac{4Q}{0.00006033}\ \text{m/s} \quad (25)$$

For D_{jet}=0.0008m ;ν=0.573 × 10^{-6}m/s

Thus $\text{Re} = \frac{\left(\frac{4Q}{0.00006033}\right) x0.0008}{\nu}$

$$= \frac{\left(\frac{4Q}{0.00006033}\right)x0.0008}{0.573 \times 10-6} = \frac{53.042Q}{0.573 \times 10-6}$$

$$Re = 92.57Qx10^6 \quad (26)$$

Where Q is calculated flow rates from experimental run.

3.7 Calculation for Nusselt Number (Nu)

The values of Nusselt Numbers are also calculated from equation 15 below,

$$Nu = \sqrt{2}\, Re^{\frac{1}{2}} * Pr^{\frac{1}{6}} * \left(\frac{kv}{kL}\right)^{\frac{1}{2}} * \left(\frac{\Delta T_{Sub}}{\Delta T_{Sat}}\right)_i^{\frac{1}{2}}$$

Then substituting equations 18, 20 and 26 into 15, yields 28

$$\text{Nu} = \sqrt{2}(0.0605)^{1/2} * (0.910)^{1/6} * 92.57Qx10^6 * \left(\frac{\Delta T_{Sub}}{\Delta T_{Sat}}\right)_i^{\frac{1}{2}} \quad (27)$$

$$Nu = 31.702 * Qx10^6 \left(\frac{\Delta T_{Sub}}{\Delta T_{Sat}}\right)^{1/2} \quad (28)$$

3.8 Calculation for Convective Heat Transfer Coefficient h

From $Nu = \frac{hD_{jet}}{k}$ (29)

Where h = convective heat transfer coefficient (w/m^2.k)

D_{jet} = diameter of impingement nozzle (m)

K = thermal conductivity of steel = 60.5 w/m,k

(John Wiley and sons. Inc., 2012)

Thus $h = \frac{KNu}{D_{jet}}$ (30)

Substituting equation 28 into 30 yields

$$h = \frac{60.5*30.717*Q*10^6*\left(\frac{\Delta T_{Sub}}{\Delta T_{Sat}}\right)_i^{\frac{1}{2}}}{D_{jet}}$$

$$= \frac{0.0605*30.717*Q*10^6*\left(\frac{\Delta T_{Sub}}{\Delta T_{Sat}}\right)_i^{\frac{1}{2}}}{0.0008} \quad (31)$$

$$h = 2322.97 * Q * 10^6 * \left(\frac{\Delta T_{Sub}}{\Delta T_{Sat}}\right)_i^{\frac{1}{2}} \quad (32)$$

Table 2: Numerical values for Prandtl Nu.,Nusselt Nu.,Reynolds Nu., and Coefficient of. Convective Heat Transfer and To for D=20mm,H=40mm and d_{jet} =0.0008mm

Prandtl.Nu $Pr = \frac{Cp\mu}{k}$	$\left(\frac{k_v}{k_L}\right)^{\frac{1}{2}}$	$\left(\frac{\Delta T_{Sub}}{\Delta T_{Sat}}\right)_i^{\frac{1}{2}}$	**Reynolds Nu.** $Re = 92.57Q * 10^6$	**Nusselt Nu.** $Nu = 31.702 * Q * 10^6 * \left(\frac{\Delta T_{sub}}{\Delta T_{sat}}\right)^{\frac{1}{2}}$	**Con.heat coeff.w/m^2,k** $h = 2322.97 * Q * 10^6 \left(\frac{\Delta T_{sub}}{\Delta T_{sat}}\right)^{\frac{1}{2}}$	Q * 10^6 m/sec	$T_o = \frac{T_1K - \Delta x(hT_\infty - 2257000V}{K - h\Delta x}$
0.91	0.2459	0.633312	801.6562	173.869	12740.29	8.66	221.4178
0.947	0.239	0.636474	1007.162	219.5312	16086.19	10.88	247.8665
0.983	0.2326	0.589768	1478.343	298.5882	21879.11	15.97	270.5271
1.03	0.2264	0.551904	694.275	131.2234	9615.418	7.5	175.1383
1.09	0.2206	0.512696	1004.385	176.3503	12922.1	10.85	220.6586
0.902	0.3561	0.8187	822.8547	230.709	16905.25	8.889	247.3771
0.878	0.3392	0.808475	1083.069	299.8741	21973.33	11.7	267.6704
0.854	0.3227	0.798549	1736.891	474.9969	34805.48	18.763	288.8938
0.843	0.303	0.769385	1322.825	348.5482	25539.94	14.29	276.9926
0.832	0.2865	0.740656	1459.181	370.1196	27120.59	15.763	279.5564

Table 3: Numerical values for Prandtl Nu.,Nusselt Nu.,Reynolds Nu., and Coefficient of. Convective Heat Transfer and To for D=45mm,H=40mm and d_{jet} =0.0008mm

Prandtl.Nu			**Reynolds Nu.**	**Nusselt Nu.**	**Con.heat coeff.w/m^2,k**		
$Pr = \frac{Cp\mu}{k}$	$\left(\frac{k_v}{k_L}\right)^{\frac{1}{2}}$	$\left(\frac{\Delta T_{sub}}{\Delta T_{sat}}\right)_i^{\frac{1}{2}}$	$Re = 92.57Q * 10^6$	$Nu = 31.702 * Q * 10^6 * \left(\frac{\Delta T_{sub}}{\Delta T_{sat}}\right)^{\frac{1}{2}}$	$h = 2322.97 * Q * 10^6\left(\frac{\Delta T_{sub}}{\Delta T_{sat}}\right)^{\frac{1}{2}}$	$Q * 10^6$ m/sec	$T_o = \frac{T_1 K - \Delta x(hT_\infty - 2257000V}{K - h\Delta x}$
0.91	0.2459	0.661717	811.8389	183.975	13480.8	8.77	228.6382
0.947	0.239	0.621423	825.7244	175.7273	12876.45	8.92	223.4117
0.983	0.2326	0.581402	1080.292	215.0968	15761.26	11.67	242.0712
1.03	0.2264	0.547981	884.0435	165.9035	12156.61	9.55	212.7263
1.09	0.2206	0.512696	707.5125	124.2254	9102.64	7.643	167.1713
0.902	0.3561	0.855315	365.3738	107.0237	7842.178	3.947	134.2699
0.878	0.3392	0.821189	480.9012	135.2432	9909.97	5.195	181.9124
0.854	0.3227	0.787222	740.56	199.6521	14629.54	8	233.4214
0.843	0.303	0.769385	875.7122	230.7394	16907.47	9.46	247.5313
0.832	0.2865	0.740656	660.9498	167.6492	12284.53	7.14	213.8687

3.9 Finite difference treatment

For 1 dimensional treatment of FD

The steps employed are: Calculating T_o for the each time period, Calculating for T_1 to T_5 using the FD^2 Calculating for A= λB + λC+Λd. The stencil for the explicit finite difference method for the heat equation of step 3 is given in fig.5

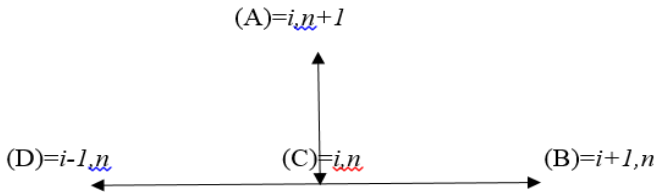

Fig 5: Stencil for explicit D.F. method of heat equation

From the stencil for the explicit finite method above, using the nodal point at (A) =i, n+1, would yield the expression

$$A = \lambda B + \lambda C + \Lambda d \quad (33)$$

By substituting the values of A, B, C, and D in equation 33, yields

$$T_{i,\,n+1} = \lambda T_{i+I,n} + (1 - 2\lambda)\, T_{i,n}) + \lambda\, T_{i-1,n} \quad (34)$$

Where $\lambda = \frac{\alpha \Delta t}{\Delta x^2}$

for steel of Mn< 0.1≤0.8% and Si ≤ 0.1%;

α = thermal diffusivity of steel=1.775 x 10^{-6} m^2/s.

(John Wiley and Sons.Inc. 2012)

3.10 Discretization of temperature development across the width

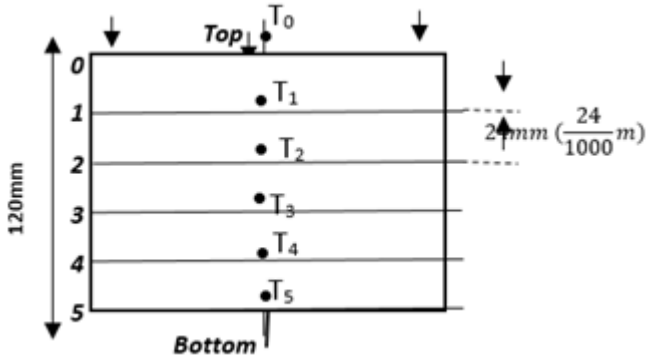

Fig 6: Sketch of temperature across the thickness from top to bottom plate

For the 1 –D"EXPLICIT F.D" to converge to a good solution; the stability is based on the conditions that

$$\{0 < \lambda \leq ½\}$$

(Crank, J., 2015)

If α = thermal diffusivity of steel = 1.775 x 10^{-6} m^2/s. For Δx = 24/1000, and Δt = 30 sec for the interval of each time used, Solving for λ in the equation 34 of

$$T_{i,\,n+1} = \lambda T_{i+I,n} + ((1 - 2\lambda)\, T_{i,n}) + \lambda\, T_{i-1,n}$$

$$\lambda = \frac{\alpha \Delta t}{\Delta x^2} = \frac{1.775\ x\ 10^{-6}\ x\ \Delta t}{0.024^2}$$

$$\lambda_{@30\ sec\ interval} = \frac{1.775\ x\ 10^{-6}\ x\ 30}{0.000576} = 0.092$$

The condition for good convergent therefore becomes

$\{0 < 0.092 \leq {}^1/_2\}$

Thus, equation 34 becomes

$$T_{i,\,n+1} = 0.092T_{i+I,n} + 0.816\ T_{i,n} + 0.092\ T_{i-1,n} \quad (35)$$

Equation 35 was then simulated using visual basic heat transfer model programme to determine the temperature distributions across the workpiece. The data obtained were used to plot and analyze the temperature history and parametric studied on the impingement heights.

3.11 Effect of Impingement Heights on Temperature Time Cooling Curve

Figure 7 and 8 show the effect of variations on impingement heights of H =40mm,50mm, 60mm and 70mm, at difference constant pipe diameters of D=20mm,25mm,32mm and 45mm respectively.

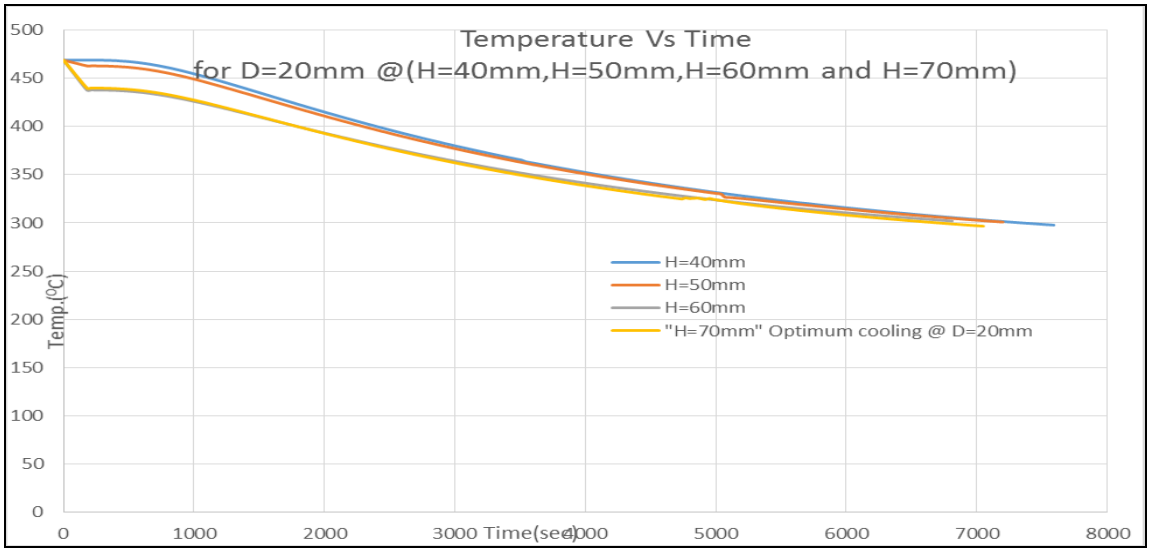

Fig 7: Effect of impingement height variations for H= 40mm, 50mm, 60mm and 70mm at constant diameter D = 20mm.

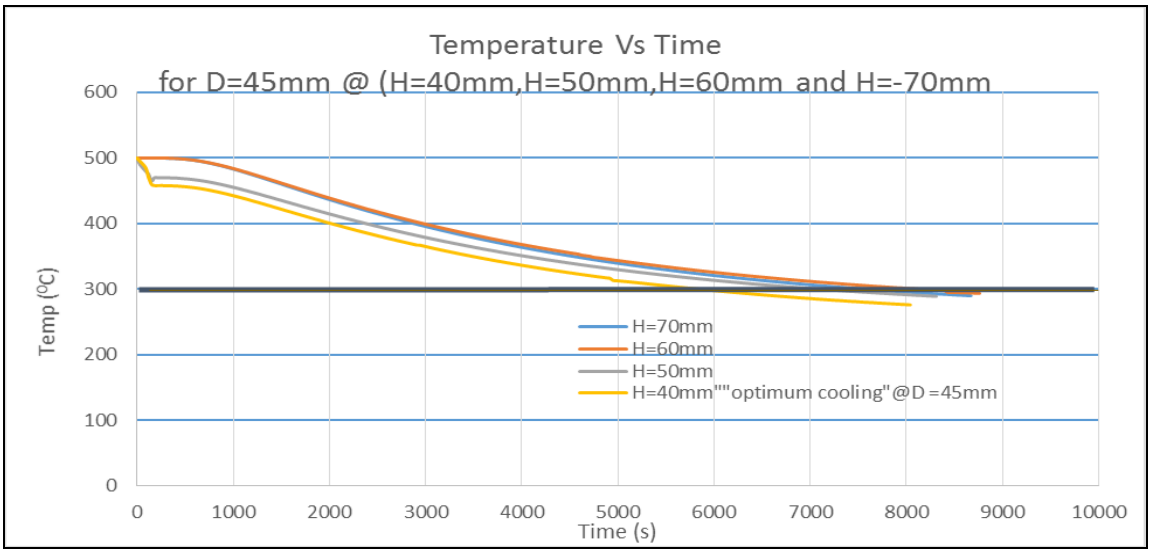

Fig 8: Effect of impingement height variations for H= 40mm, 50mm, 60mm and 70mm at constant diameter D = 45mm.

Result Discussion and Conclusion

The effect of differnect in impingement height shows that for Figure 7 of D=20mm at impingement height of H=70mm and Fig 8 of D=45mm, of impingement height 40mm were compared for the parametric studies, with a controlled temperature cooling of 300^0C.However, with Fig 7, the optimum cooling occurred at D= 20mm with impingement height of 70mm at a controlled temperature cooling of 300^0C. With daimeter D= 45mm the optimum cooling was recorded at lowest height of H= 40mm.This comparism depicts that the smaller the pipe diameter, the faster cooling with high impingement height but with bigger pipe diameter the cooling is better with smaller daimeter pipe. This could be as a result of stresmwise velocity Webb and Ma, (1995), that water velocity for planar or water curtin jet does not decrease, whereas water velocity in parallel flow zone of circular jets deceases.

References

1. Azon. *www.azon.co/article.aspex*? Article 10.6118. Mechanical Properties of Low Carbon Steel of AISI. 2012, 1018.
2. Dhir VK. *Boiling heat transfer*, Annual Review of Fluid Mechanics. 1998; 30:365-401.
3. Filipovic J. Ph.D. Thesis, Purdue University, 1994.
4. John Wiley, Sons Inc. Fundamentals of Heat and Mass Transfer Six Editions: Thermo, 2012.
5. Physics Properties of Thermal Conductivity of Liquids and Vapours, Table A-6.
6. John Wiley and Sons, Inc. *Fundamentals of Heat and Mass Transfer Sixth Edition*, India Edition: Thermo Physics Properties of liquid and Vapour Table A-4, 2012.
7. John Wiley and Sons Inc. *Fundamentals of Heat and Mass Transfer, Sixth Edition*: Thermophysics Properties of Selected Metallic Solids Table A-1, 2012.

8. Li D. Boiling Water Heat Transfer during Quenching on Steel Plates and Tubes, Ph.D Thesis, MMAT, UBC.
9. Liu, Z.H. (2015). Prediction of Minimum Heat Flux for Water Jet Boiling on a Hot Plate, J. Thermo physics and Heat Transfer. 2003; 17(2):159-165.
10. Sergners JV, Watons TTR. Jourals of Physical, and Chemicals Reference Data for Viscosity and thermal Conductivity, Table A-9, 1995.
11. Sengers JS, Watson TTR. Journals of Physical and Chemical Reference Data, Properties of Temperature and Prandtl Nu. Tables A-9 Appnedix, 1995.
12. Webb, BW, Ma CF. Single-Phase liquid Jet Impingement Heat Transfer.*In.J.P.Harttuett. Advances in Heat Transfer*. Vol.26, PP.105- 215, Academic Press, New York, 1995.
13. Wolf DH, Incropera FP, Viskanta R. Advances in Heat Transfer. 1993; 23:1-131.
14. Tong LS, Tang YS. Boiling Heat Transfer and Two-phase Flow, 2nd ed., Taylor and Francis, Washington, DC. 1997, 1-10.